Clinical Science (2024) **138** 371–385
https://doi.org/10.1042/CS20230973

PORTLAND PRESS

Research Article

Loss of FoxO1 activates an alternate mechanism of mitochondrial quality control for healthy adipose browning

Limin Shi[1,2,3,*], Jinying Yang[1,2,*], Zhipeng Tao[4,5], Louise Zheng[4], Tyler F. Bui[1], Ramon L. Alonso[1], Feng Yue[6] and Zhiyong Cheng[1,2,3,4,*]

[1]Department of Food Science and Human Nutrition, University of Florida, Gainesville, FL 32611, U.S.A.; [2]Interdisciplinary Nutritional Sciences Doctoral Program, Center for Nutritional Sciences, University of Florida, Gainesville, FL 32611, U.S.A.; [3]Center for Integrative Cardiovascular and Metabolic Diseases, University of Florida, Gainesville, FL 32610, U.S.A.; [4]Department of Human Nutrition, Foods, and Exercise, Virginia Tech, Blacksburg, VA 24061, U.S.A.; [5]Cutaneous Biology Research Center, Massachusetts General Hospital, Harvard Medical School, Charlestown, MA 02129, U.S.A.; [6]Department of Animal Sciences, University of Florida, Gainesville, FL 32611, U.S.A.

Correspondence: Zhiyong Cheng (z.cheng@ufl.edu)

Browning of white adipose tissue is hallmarked by increased mitochondrial density and metabolic improvements. However, it remains largely unknown how mitochondrial turnover and quality control are regulated during adipose browning. In the present study, we found that mice lacking adipocyte FoxO1, a transcription factor that regulates autophagy, adopted an alternate mechanism of mitophagy to maintain mitochondrial turnover and quality control during adipose browning. Post-developmental deletion of adipocyte FoxO1 (adO1KO) suppressed Bnip3 but activated Fundc1/Drp1/OPA1 cascade, concurrent with up-regulation of Atg7 and CTSL. In addition, mitochondrial biogenesis was stimulated via the Pgc1α/Tfam pathway in adO1KO mice. These changes were associated with enhanced mitochondrial homeostasis and metabolic health (e.g., improved glucose tolerance and insulin sensitivity). By contrast, silencing Fundc1 or Pgc1α reversed the changes induced by silencing FoxO1, which impaired mitochondrial quality control and function. Ablation of Atg7 suppressed mitochondrial turnover and function, causing metabolic disorder (e.g., impaired glucose tolerance and insulin sensitivity), regardless of elevated markers of adipose browning. Consistently, suppression of autophagy via CTSL by high-fat diet was associated with a reversal of adO1KO-induced benefits. Our data reveal a unique role of FoxO1 in coordinating mitophagy receptors (Bnip3 and Fundc1) for a fine-tuned mitochondrial turnover and quality control, underscoring autophagic clearance of mitochondria as a prerequisite for healthy browning of adipose tissue.

Introduction

Adipose tissues have a high plasticity that is essential to metabolic homeostasis [1,2]. In response to stimuli, white adipose tissues may undergo transdifferentiation to acquire a browning phenotype, which is characterized by increased mitochondrial content and reduced adipocyte size [1–3]. Adipose browning is associated with an upregulation of mitochondrial uncoupling proteins 1 (UCP1), which facilitates energy expenditure through thermogenesis [1]. In obese individuals, white adipose tissues are less responsive to browning stimuli, which may account for the compromised plasticity and metabolism [4,5]. As such, development of strategies to stimulate adipose browning has the potential to unravel new anti-obesity options.

Mitochondria are the hub of energy metabolism and thermogenesis in adipose tissue [1]. The quality control of mitochondria is regulated by several factors that mediate mitochondrial biogenesis (e.g., Pgc1α and Tfam), dynamics (e.g., Mfn1, Mfn2, OPA1, and Drp1), and autophagic clearance or mitophagy (e.g.,

[*]These authors contributed equally to this work.

Received: 25 August 2023
Revised: 26 February 2024
Accepted: 27 February 2024

Accepted Manuscript online: 28 February 2024
Version of Record published: 12 March 2024

Clinical Science (2024) **138** 371–385
https://doi.org/10.1042/CS20230973

Pink1/parkin, Bnip3, and Fundc1) [1,6]. In addition, dynamic proteins (e.g., OPA1, Drp1, and Mfn2) may interact with mitophagy proteins (e.g., Fundc1 and Pink1/parkin) and facilitate mitochondrial clearance via autophagy [6,7]. Dysregulated mitochondrial biogenesis and dynamics have been implicated in diseased conditions [8,9], while the role of autophagy or mitophagy in metabolic regulation remains to be established. For instance, autophagic activity is found essential to support skeletal muscle plasticity in response to endurance exercise [10], whereas autophagy deficiency due to skeletal muscle-specific deletion of Atg7 improves systemic metabolism and protects against diet-induced obesity and insulin resistance [11]. In adipose tissue, blockage of autophagic and mitophagic activity increases mitochondrial density, which either enhances or compromises systemic metabolism [12–15]. Moreover, embryonic ablation of Atg7 in adipose tissue increases mouse mortality rate at young ages regardless of the browning effects [14], and dysfunctional mitochondria are accumulated in mice that have post-developmental deletion of Atg3 and Atg16L1 [12]. The controversies may arise from confounding factors such as off-target DNA recombination mediated by aP2-Cre and compromised lineage plasticity during embryonic gene deletion [2,12]. Regardless, these studies underscore the necessity of further investigation of mitophagy during adipose browning, and one of the critical questions remains as to whether and how mitochondrial turnover can be maintained for mitochondrial quality control in adipocytes if autophagic clearance of mitochondria is blocked.

FoxO1 is a transcription factor conserved across species and has been shown to regulate mitochondria, autophagy, and metabolism [6,16,17]. Hyperactive FoxO1 in the liver dysregulates mitochondrial function and leads to metabolic disorders in mice, but ablation of FoxO1 reverses mitochondrial and metabolic abnormalities [18,19]. In mitophagy, FoxO1 may control the formation and maturation of autophagosome through *Atg* genes, mediate the processes of mitochondria being connected to and engulfed by autophagosome through adaptors Pink1/parkin or receptor Bnip3, and regulate lysosomal CTS enzymes [6,17]. We and others have shown that silencing FoxO1 or overexpressing an inactive FoxO1 mutant in adipose tissue leads to a browning phenotype [2,20], which is associated with increased mitochondrial density and iron content in adipocytes [2]. However, it is unknown how mitochondrial turnover is regulated during adipose browning. In the present study, we found that post-developmental deletion of adipose FoxO1 elicited an alternate mechanism of mitochondrial quality control by differentially regulating Fundc1 and Bnip3 for mitophagy and activating mitochondrial biogenesis via Pgc1α, which sustained mitochondrial function and metabolic health during adipose browning. By contrast, blockage of mitophagy (via Atg7, Fundc1, or CTSL) or mitochondrial biogenesis (via Pgc1α) caused mitochondrial dysfunction and metabolic disorders. Our data suggest that a fine-tuned mitochondrial quality control is required for healthy browning of adipose tissue.

Materials and methods

Mice

FoxO1$^{flox/flox}$, Atg7 $^{flox/flox}$, and AdipoqCreER^{T2} mice were described previously [18,21–23]. To obtain AdipoqCreER^{T2}:: FoxO1$^{flox/flox}$ and AdipoqCreER^{T2}:: Atg7 $^{flox/flox}$ mice, we crossed male AdipoqCreER^{T2} mice with female FoxO1$^{flox/flox}$ and Atg7 $^{flox/flox}$ mice, respectively. To induce post-developmental deletion of FoxO1 and Atg7, adult AdipoqCreER^{T2}:: FoxO1$^{flox/flox}$ mice and AdipoqCreER^{T2}:: Atg7 $^{flox/flox}$ mice (13- to 15-week-old) were treated with tamoxifen (50 mg/kg body weight) by intraperitoneal injection once a day for 5 consecutive days [24]. Age-matched FoxO1$^{flox/flox}$ and Atg7 $^{flox/flox}$ were treated with tamoxifen likewise and used as the control mice. All the mice were housed in plastic cages on a 12-h (7:00 am to 7:00 pm) light–dark photocycle, with free access to water and regular chow diet. Measurement of body composition with a Bruker Minispec NMR Analyzer (Bruker Optics, Billerica, MA, U.S.A.) and body temperature with a TH5 thermometer (Physitemp, Clifton, NJ) were conducted as described [2]. When applicable, the mice were fed on a regular chow or high-fat diet (HFD, 60% kcal from fat, Research Diet, D12492i) for the indicated durations. The mice were killed by inhalation of CO_2, followed by tissue collection for molecular analysis. The procedures of mouse handling and treatments were performed at the animal facilities at the University of Florida (UF) and Virginia Tech (VT), by following the protocols approved by the Institutional Animal Care and Use Committees at UF and VT.

Immunohistochemistry

Adipose tissues were fixed with 10% formalin. The fixed tissues were embedded in paraffin, and 7 μm sections were prepared for immunohistochemical analysis of UCP1. Briefly, paraffin was removed from the adipose tissue sections with xylene and rehydrated with a series of alcohol solutions. The sections were immersed in a preheated citrate buffer solution at 95°C for 20 min for heat-induced epitope retrieval. Then the sections were treated with hydrogen peroxide solution to mask the activity of endogenous peroxidase. Immunostaining followed a standard protocol using a UCP1

antibody (PA5-29575 from ThermoFisher or UCP1 antibody (23673-1-AP) from Proteintech) and Diaminobenzidine (DAB) peroxidase substrate kit (SK-4105) from Vector Laboratory. Images were taken with a Nikon Eclipse Ts2 microscope (Melville, NY, U.S.A.).

Transmission electron microscopy

TEM was conducted as described previously [2]. Specifically, adipose tissues were cut into small pieces (∼1 mm^3) and fixed in 2.5% glutaraldehyde in sodium cacodylate buffer and post fixed in 1% osmium tetroxide and embedded in an Epon-Araldite mixture. Ultrathin (80 nm) sections were obtained with an Ultracut E ultramicrotome and post-stained with 3% uranyl acetate, followed by 0.4% lead citrate. The ultrathin sections were examined with a JEOL 1200EX transmission electron microscope and images were recorded digitally.

Cell culture and mitochondrial membrane potential

3T3L1 cells (CL-173™, ATCC) were cultured and induced for differentiation as described previously [2,25]. When applicable, the preadipocytes and adipocytes were treated for 3–4 days with vehicle (DMSO), FoxO1 inhibitor AS1842856 (1 μM), autophagy inhibitor Bafilomycin A1 (0.1 μM), and siRNAs against Pgc1α, Fundc1, and Atg7 using Lipofectamine® RNAiMAX Reagent (cat # 13778150, ThermoFisher) [26]. Then the cells were assessed by high-resolution respirometry (Oxygraph-2k, Oroboros). In addition, the cells were stained by Membrane Potential Indicator (CB-80600, Codex BioSolutions Rockville, MD) for 30 min according to the manufacturer's instruction, followed by fluorescence imaging on a Nikon Eclipse Ts2-FL Inverted Microscope, or fluorescence reading on a Synergy LX. Multi-Mode Microplate Reader (BioTek, VT). The ratio of red fluorescence to green fluorescence indicates the status of mitochondrial membrane potential [27].

Respirometry

Respiration was assessed by high resolution respirometry (Oxygraph-2k, Oroboros) as described previously [2]. Briefly, 3T3L1 cells (5×10^4 preadipocytes; 6×10^5 adipocytes) were suspended in 2.1 mL mitochondrial respiration medium (Oxygraph-2k, Oroboros). Basal cellular respiration was recorded after the injection of pyruvate (5 mM), and proton leak respiration was recorded after injection of oligomycin (10 ng/mL). Maximal cellular respiration rates were measured by titration of carbonyl cyanide 4-(trifluoromethoxy) phenylhydrazone (FCCP, 0.5-μM steps). Nonmitochondrial oxygen consumption was determined after injection of antimycin A (2.5 μM), and it was subtracted from all other respiratory states [28,29].

GTT and HOMA-IR

Glucose tolerance test (GTT) and insulin tolerance test (ITT) were performed as described previously [2,30]. For GTT, the mice were fasted overnight (∼14 h), and the animals were injected intraperitoneally with D-glucose (2 g/kg of body weight), and blood glucose was measured at the indicated time points with Contour Blood Glucose Meters and Test Strips. For homeostasis model index of insulin resistance (HOMA-IR), ultra-sensitive mouse insulin ELISA kits were used to measure insulin in plasma from overnight-fasted mice according to the manufacturer (Crystal Chem, Elk Grove Village, IL); glucose was measured with Contour Blood Glucose Meters and Test Strips for overnight-fasted mice. HOMA-IR was calculated as follows [31]: HOMA-IR = insulin (mU/L) × glucose (mg/dL)/405, or HOMA-IR = insulin (mU/L) × glucose (mmol/L)/22.5.

Iron assay

Total non-heme iron was analyzed with Iron Assay Kits (Cat # MAK025) from Sigma, according to the manufacturer's instructions [2,32,33].

RNASeq

Total RNA from adipose tissue was prepared with RNeasy Mini Kits (Qiagen), and mRNA was purified from total RNA using poly-T oligo-attached magnetic beads [2]. After library construction, diluting library to 1.5 ng/μL with the preliminary quantitative result by Qubit2.0 and detecting the insert size by Agilent 2100. Q-PCR was used to accurately quantify the library effective concentration (>2 nM), in order to ensure the library quality. Libraries were fed into Illumina machine (Illumina Platform PE150) after pooling according to activity and expected data volume. Raw image data file from high-throughput sequencing was transformed to Sequenced Reads (Raw Reads) by CASAVA base recognition (Base Calling). Raw reads were filtered to remove reads containing adaptors, or >10% bases that could not be determined, or when the Qscore of over 50% bases were ≤5. STAR was sued to map the clean reads

Clinical Science (2024) **138** 371–385
https://doi.org/10.1042/CS20230973

to the reference genome (Mus MusculusGRCm38/mm10). Differential expression analysis was performed with a DESeq2 R package and enrichment analysis with ClusterProfiler [2].

Immunoblotting

The procedure was performed as described [2,25]. Specifically, tissue and cell lysates were prepared with PLC lysis buffer (30 mM Hepes, pH 7.5, 150 mM NaCl, 10% glycerol, 1% Triton X-100, 1.5 mM $MgCl_2$, 1 mM EGTA, 10 mM NaPPi, 100 mM NaF, 1 mM Na_3VO_4) supplemented with protease inhibitor cocktail (Roche) and 1 mM PMSF. Total protein concentrations of the lysates were determined using a DC protein assay kit (Bio-Rad). Antibody (catalog number) information: GAPDH (600004-1-lg), Fundc1 (28519-1-AP), CTSL (66914-1-1g), Pink1 (23274-1-AP), Pgc1α (66369-1-lg), Mfn1 (13798-1-AP), Drp1 (12957-1-AP), Tfam (22586-1-AP), LC3 (14600-1-AP), UCP1 (23673-1-AP), FoxO3 (10849-1-AP), and OPA1 (27733-1-AP) antibodies were purchased from Proteintech (Rosemont, IL, U.S.A.); FoxO1 (9454s), Atg7 (8558s), acetyl-lysine (9441s), and α-Tubulin (2125) antibodies from Cell Signaling Technology (Beverly, MA, U.S.A.).

Statistical analysis

Measurements were duplicated or triplicated, with 6–12 mice included in each group. Data were presented as mean ± SD. Unless the use of female mice were specified, the animal studies were conducted on males. Differences between groups and treatments were validated by one-way analysis of variance or a two-sided *t*-test. A value of $P<0.05$ was considered statistically significant.

Results

Mitochondrial turnover is sustained during adipose browning induced by post-developmental deletion of FoxO1

Given the confounding effects of off-target DNA recombination and embryonic deletion of target genes on lineage plasticity during embryonic development [12,34–38], we generated inducible post-developmental adipose FoxO1 knockout (adO1KO) mice [2] by crossing adipocyte-specific AdipoqCreER^{T2} mice [12,23] with FoxO1-floxed mice [18,21] (see genotyping details in Supplementary Figure S1A,B). In line with previous studies [2], the adO1KO mice fed on regular chow diet exhibited metabolic enhancement in comparison with the control mice, such as increased glucose-handling capacity assessed by glucose tolerance test (Figure 1A,B) and improved insulin sensitivity assessed by homeostasis model index of insulin resistance HOMA-IR (the lower HOMA-IR, the higher insulin sensitivity) (Figure 1C). The metabolic improvements were concurrent with adipose browning phenotype in adO1KO mice, including the up-regulation of UCP1, smaller adipocyte size, and elevated thermogenesis and body temperature (Figure 1D–F). As both male (Figure 1A–F) and female (Supplementary Figure S1C–I) mice showed similar phenotype, we focused on males in the following studies.

Examination of the ultrathin section of inguinal adipose tissue using transmission electron microscopy (TEM) suggested that the number of mitochondria in autophagosome (MiA, i.e., autophagic clearance of mitochondria, marked by arrows) in adO1KO mice was comparable with that in the control mice, but the population of mitochondria outside autophagosome (MoA, marked by asterisks) was significantly elevated in adO1KO mice (Figure 1G,H). Western blotting and densitometric analyses of autophagy proteins showed that deletion of FoxO1 in adipose tissue (adO1KO) up-regulated Atg7 (the key regulator of autophagosome formation and maturation) [39] and CTSL (the key lysosomal enzyme for cargo clearance) [40,41], which was concurrent with sustained conversion of LC3I (i.e., lipidation of LC3I) to LC3II to facilitate autophagosome formation and maturation (Figure 1I–K). Thus, adipose browning due to post-developmental deletion of adipocyte FoxO1 is associated with sustained mitophagic activity and increased mitochondrial content during adipose browning.

Post-developmental deletion of FoxO1 reciprocally regulates Fundc1 and Bnip3 and activates mitochondrial biogenesis

To further investigate how adO1KO regulates mitochondrial turnover and homeostasis, we analyzed adaptor-dependent (e.g., Pink1) and receptor-dependent (e.g., Bnip3 and Fundc1) mitophagy pathways as well as mitochondrial biogenesis (e.g., Pgc1α and Tfam) [6,16,42,43]. Interestingly, ablation of FoxO1 reciprocally regulated Bnip3 (down-regulated by 63%, $P<0.01$) and Fundc1 (up-regulated by 3.4-fold, $P<0.001$), although Pink1 was comparable in adO1KO and control mice (Figure 2A,B). In line with the notion that Fundc1-dependent mitophagy requires Drp1 and OPA1 to facilitate mitochondria being connected to and engulfed by autophagosomes

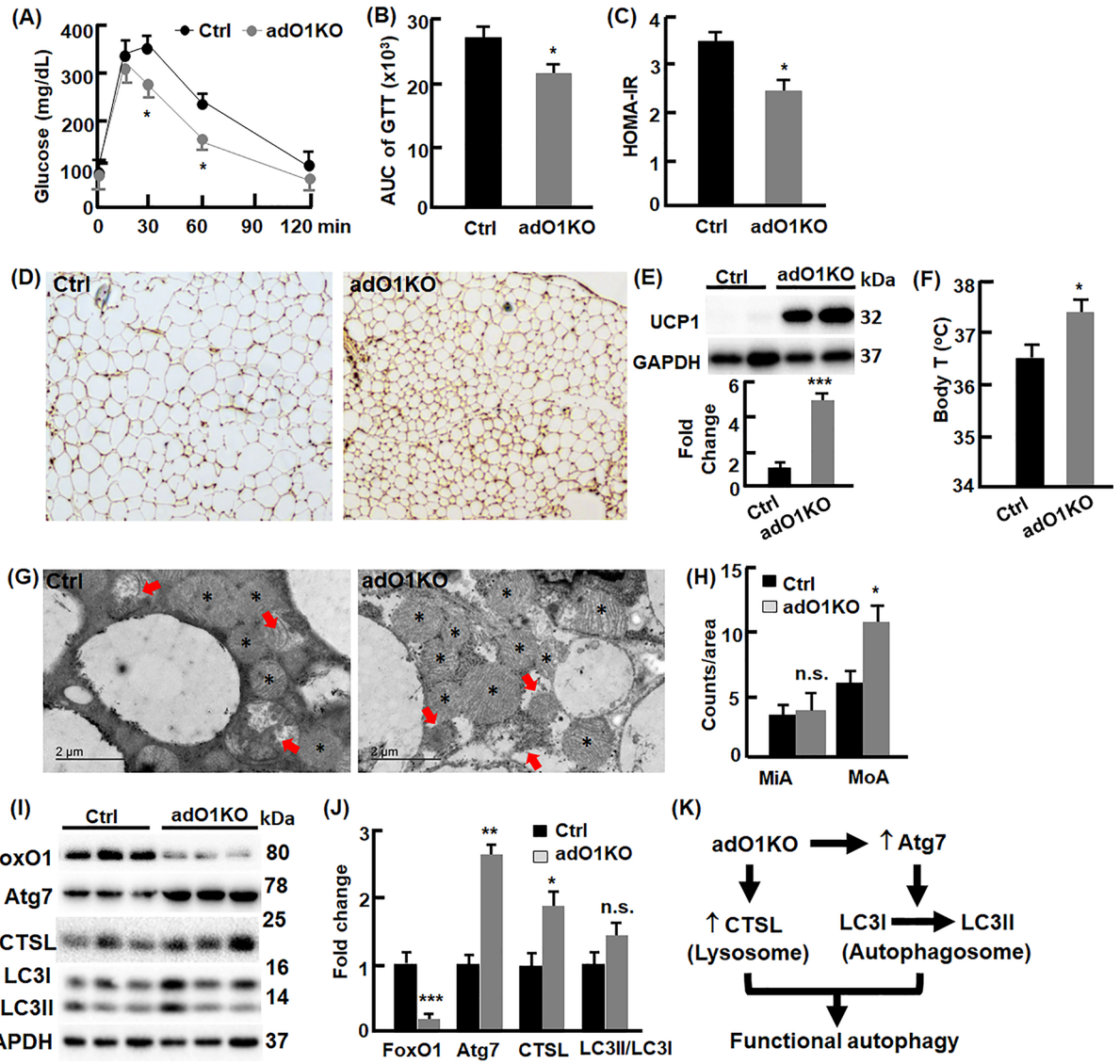

Figure 1. Post-developmental deletion of FoxO1 induces adipose browning without blocking mitochondrial turnover in mice fed on regular chow diet

(**A,B**) Glucose tolerance test and calculation of area under the curve (AUC) for control (Ctrl) and adO1KO mice; n=6–8. (**C**) Measurement of homeostasis model index of insulin resistance (HOMA-IR); n=8–12. (**D–E**) Analyses of UCP1 proteins in inguinal adipose tissues by immunohistochemistry (panel D, magnification, 200×) and Western blotting followed by densitometric analyses (E, n=6). (**F**) Measurement of body temperatures; n=6–8. (**G**) Transmission electron microscopic view of inguinal adipose tissue sections. The arrows point to mitochondria engulfed by autophagosome for clearance, and the asterisks mark the mitochondria not engulfed by autophagosome. (**H**) Counts of mitochondria inside autophagosome (MiA, marked by arrows) and mitochondria outside autophagosome (MoA, marked by asterisks) under the transmission electron microscope (area of 35 μm^2); n=6–8. (**I,J**) Western blotting (**I**) and densitometric (**J**) analyses of FoxO1 and autophagy proteins; n=6. (**K**) Schematic view of how autophagic activity was sustained in adO1KO mice; $^*P<0.05$, $^{**}P<0.01$, $^{***}P<0.001$; n.s., not significant.

for autophagic clearance (Figure 2C) [44], we found that Drp1 (by 2.1-fold, $P<0.05$) and OPA1 (by 2.7-fold, $P<0.05$) were both elevated significantly but Mfn1 was marginally changed (Figure 2D,E). Additionally, the key regulator of mitochondrial biogenesis Pgc1α and its downstream effector Tfam were both up-regulated by post-developmental deletion of FoxO1, supporting the notion that silencing FoxO1 activates Pgc1α-mediated mitochondrial biogenesis [18,45,46] (Figure 2F,G). These results suggest that the adO1KO mice adopt an alternate autophagic pathway, where Fundc1/OPA1/Drp1 cascade dominates over Pink1 and Bnip3 pathways, to sustain mitochondrial turnover;

Clinical Science (2024) **138** 371–385
https://doi.org/10.1042/CS20230973

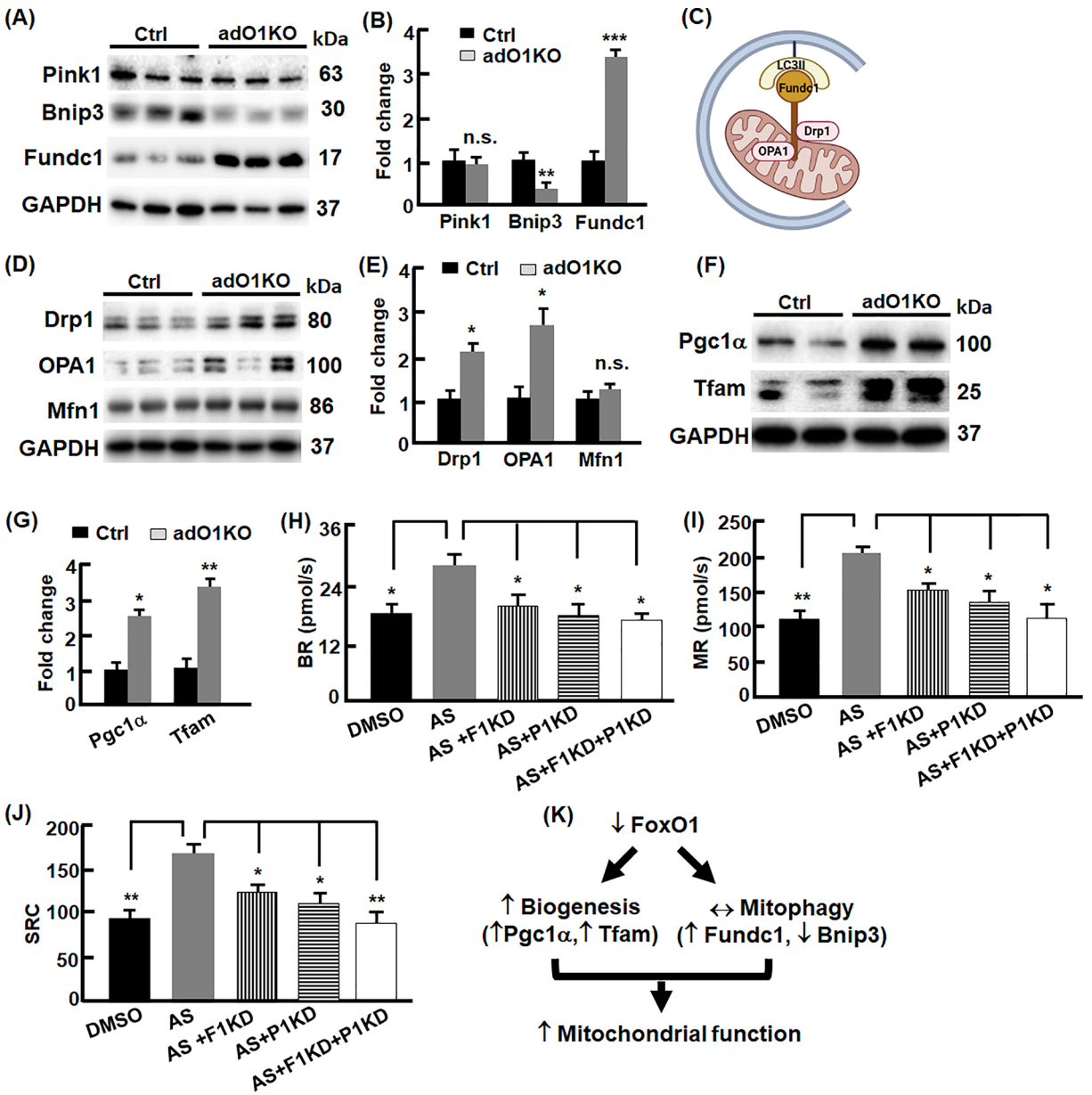

Figure 2. Post-developmental deletion of adipocyte FoxO1 activates alternate mitophagy pathways and mitochondrial biogenesis in mice fed on regular chow diet

(**A,B**) Western blotting (A) and densitometric (B) analyses of mitophagy adaptor and receptor proteins; n=6. (**C**) Illustration of the partnership between Fundc1 with Drp1 and Opa1 in connecting mitochondria to and engulfed by autophagosome via LC3II. (**D,E**) Western blotting (D) and densitometric (E) analyses of mitochondrial dynamics proteins Drp1, OPA1, and Mfn1; n=6. (**F,G**) Western blotting (F) and densitometric (G) analyses of markers of mitochondrial biogenesis; n=6. (**H–J**) Measurement of basal respiration (BR, H), maximal respiration (MR, I), and spare respiration capacity (SRC, J) of 3T3L1 adipocytes; n=3–4. DMSO stands for the vehicle, AS for FoxO1 inhibitor AS1842856, F1KD for Fundc1 knockdown, and P1KD for Pgc1α knockdown. (**K**) Schematic view of how silencing FoxO1 activates mitochondrial biogenesis and sustains mitochondrial turnover to enhance mitochondrial function. *P<0.05, **P<0.01, ***P<0.001; n.s., not significant.

the stimulated mitochondrial biogenesis may account for the increase mitochondrial density in adO1KO mice (Figure 1F,G). To assess how silencing FoxO1 affects mitochondrial function, we measured cell respiration in 3T3L1 adipocytes (Figure 2H–J), showing that FoxO1 inhibition by the specific antagonist AS1842856 (shortened as AS) caused a significant increase in basal (BR) and maximal (MR) respiration (Figure 2H,I). Consistently, mitochondrial

spare respiration capacity (SRC) was enhanced by 94.5% ($P<0.01$) by AS (Figure 2J). A similar phenotype was observed in 3T3L1 preadipocytes, where both membrane potential and respiration were enhanced by FoxO1 inhibition (Supplementary Figure S2). However, knockdown of Pgc1α (P1KD), Fundc1 (F1KD), or both, reversed the effects of FoxO1 inhibition on respiration (Figure 2H–J; Supplementary Figure S2E–G). These data suggest that silencing FoxO1 enhances mitochondrial metabolism and elicits an alternate mechanism of mitochondrial quality control via Fundc1 (mitophagy) and Pgc1α (mitochondrial biogenesis) (Figure 2K).

Post-developmental blockage of autophagy compromises mitochondrial turnover and function and metabolism

Atg7 may regulate selective (e.g., Fundc1-dependent) and nonselective clearance of mitochondria by controlling autophagosome formation and maturation [39]. The observation of Atg7 upregulation by post-developmental adO1KO (Figure 1I,J) prompted us to examine how blocking both selective and nonselective mitochondrial clearance affects mitochondrial and metabolic homeostasis. We generated post-developmental adipose Atg7 knockout (ad7KO) mice by crossing adipocyte-specific AdipoqCreER^{T2} mice [23] with Atg7-floxed mice [22]. As shown in Figure 3A,B, deletion of Atg7 from adipocytes was effective (by 81%, $P<0.001$), which was associated with drastic down-regulation of CTSL (by 53%, $P<0.05$) and inhibition of LC3I to LC3II conversion (91%, $P<0.001$), leading to significant accumulation of LC3I and decrease of LC3II/LC3I ratio, indicative of massive blockade of autophagy [47]. Examination of the ultrathin sections of adipose tissues using TEM revealed a lower mitophagic activity (MiA, marked by arrows) and a higher mitochondrial content (MoA, marked by asterisks) in ad7KO mice (Figure 3C,D). Mitochondrial UCP1, the hallmark of adipose browning [1], was up-regulated by 2.2-fold ($P<0.01$, Figure 3E). These results suggest that post-developmental deletion of Atg7 induced a browning phenotype, which was further confirmed by RNA sequencing analysis, showing the up-regulation of *Cidea*, mitochondrial genome encoded genes (e.g., *mt-Nd1*, *mt-Nd2*, *mt-Nd3*, *mt-Nd4*, and *mt-Cytb*), and iron status marker *Fth1* (Figure 3F). Indeed, non-heme iron content was increased in adipose tissue from ad7KO mice (Supplementary Figure S3A), as observed during the browning process of adipose tissue in adO1KO mice [2]. In line with the browning phenotype, the gene related to mitochondrial fatty acid oxidation (e.g., *Acsm3*) was elevated while the genes involved in fatty acid synthesis (e.g., *Acaca and Fasn*) were down-regulated in Ad7KO mice (Figure 3F), which was associated with a higher thermogenic activity indicated by body temperature (Figure 3G). Intriguingly, deletion of adipose Atg7 led to metabolic disorders, including impaired glucose tolerance and reduced insulin sensitivity (Figure 3H–J), although significant changes were not observed in fat mass, body weight, or food intake (Supplementary Figure S3B–D). Knockdown of Atg7 (Atg7-KD; Figure 3K) in adipocytes significantly impaired basal respiration (BR; $P<005$; Figure 3L), maximal respiration (MR; $P<0.05$; Figure 3M), and mitochondrial spare respiration capacity (SRC; $P<0.05$; Figure 3N), in line with the metabolic derangements observed in Atg7-deficient mice (Figure 3H–J). Thus, Atg7-mediated autophagy or mitophagy is critical for mitochondrial and metabolic health (Figure 3O), suggesting that a healthy browning of adipose tissue requires robust mitophagy for mitochondrial quality control.

High fat diet (HFD) blocks lysosomal activity and overrides adO1KO-induced metabolic benefits

To examine whether adO1KO-induced adipose browning protects the mice from diet induced metabolic disorders, we treated the mice with HFD per two strategies (Figure 4A), CTH (i.e., chow → tamoxifen → HFD) and HTH (i.e., HFD → tamoxifen → HFD). CTH was to examine whether adO1KO prevents the development of obesity and metabolic disorders fed on HFD, and HTH to determine whether adO1KO reverses existing obesity and metabolic derangements. Intriguingly, body weight and fat mass were comparable between adO1KO and control mice in both CTH and HTH feeding strategies (Figure 4B,C). Moreover, adO1KO mice fed on HFD showed marginal improvement of metabolism compared with the control mice (Figure 4D,E), suggesting that HFD overrides adO1KO-induced metabolic benefits observed with chow diet (Figure 1A–C; Supplementary Figure S1A–E). Indeed, adO1KO-induced changes in Atg7, Bnip3, and Fundc1 in mice on chow diet (Figures 1I,J and 2A,B) were absent in mice on HFD (Figure 4F–I), presumably because FoxO3 was activated via deacetylation and compensated for the loss of FoxO1 [48,49] (Supplementary Figure S4). In addition, the lysosomal enzyme CTSL was down-regulated in adO1KO mice fed on HFD (Figure 4F,G), consistent with the notion that HFD dysregulates CTSL and causes dysfunctional lysosomes or autolysosomes [40]. Notably, the upregulation of the browning marker UCP1 was sustained in adO1KO mice on HFD, at least in part due to mitigated clearance of mitochondria via autophagy that causes accumulation of dysfunctional mitochondria [12] (Figure 4J). In line with this, blocking autophagy by Bafilomycin A1 (shortened as Baf), the inhibitor of lysosome function and autophagosome–lysosome fusion [50,51], abolished the mitochondrial

Clinical Science (2024) **138** 371–385
https://doi.org/10.1042/CS20230973

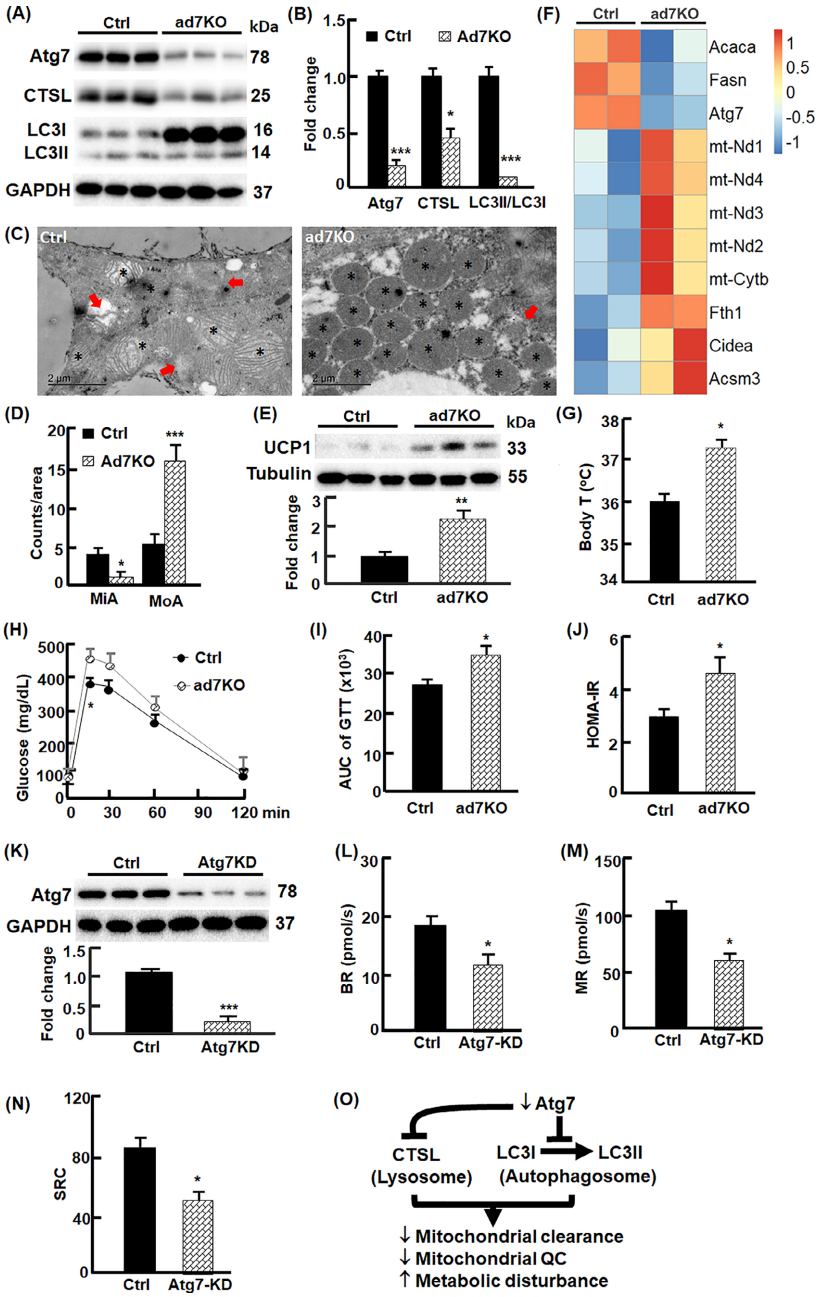

Figure 3. Post-developmental ablation of autophagy via Atg7 reduces mitochondrial turnover and causes metabolic disorders in mice fed on regular chow diet

(**A,B**) Western blotting (A) and densitometric (B) analyses of autophagy proteins in control (Ctrl) and adipocyte Atg7 knockout (ad7KO) mice; n=6. (**C**) Transmission electron microscopic view of inguinal adipose tissue sections. The arrows point to mitochondria engulfed by autophagosome for clearance, and the asterisks mark the mitochondria not engulfed by autophagosome. (**D**) Counts of mitochondria inside autophagosome (MiA, marked by arrows) and mitochondria outside autophagosome (MoA, marked by asterisks) under the transmission electron microscope (area of 35 μm^2); n=6–8. (**E**) Western blotting (upper panel) and densitometric (lower panel) analyses of adipose browning maker UCP1 in inguinal adipose tissues; n=6. (**F**) RNAseq analysis of Atg7, mitochondrial genes (mt-Nd1, mt-Nd2, mt-Nd3, mt-Nd4, mt-cytb), fatty acid metabolism related genes (Fasn, Acaca, and Acsm3), browning marker (Cidea), and iron status marker (Fth1) in Ctrl and ad7KO mice. (**G**) Measurement of body temperatures; n=6. (**H,I**) Glucose tolerance test (H) and calculation of area under the curve (AUC, I); n=6–8. (**J**) Measurement of HOMA-IR; n=6–10. (**K**) Knockdown of Atg7 (Atg7-KD) in 3T3L1 cells; n=4–6. (**L–N**) Measurement of basal respiration (BR, L), maximal respiration (MR, M), and spare respiration capacity (SRC, N) of 3T3L1 adipocytes; n=3–4. (**O**) Schematic view of how blockage of autophagy via Atg7 impaired mitochondrial turnover and metabolic function; QC, quality control. *P<0.05, **P<0.01, ***P<0.001.

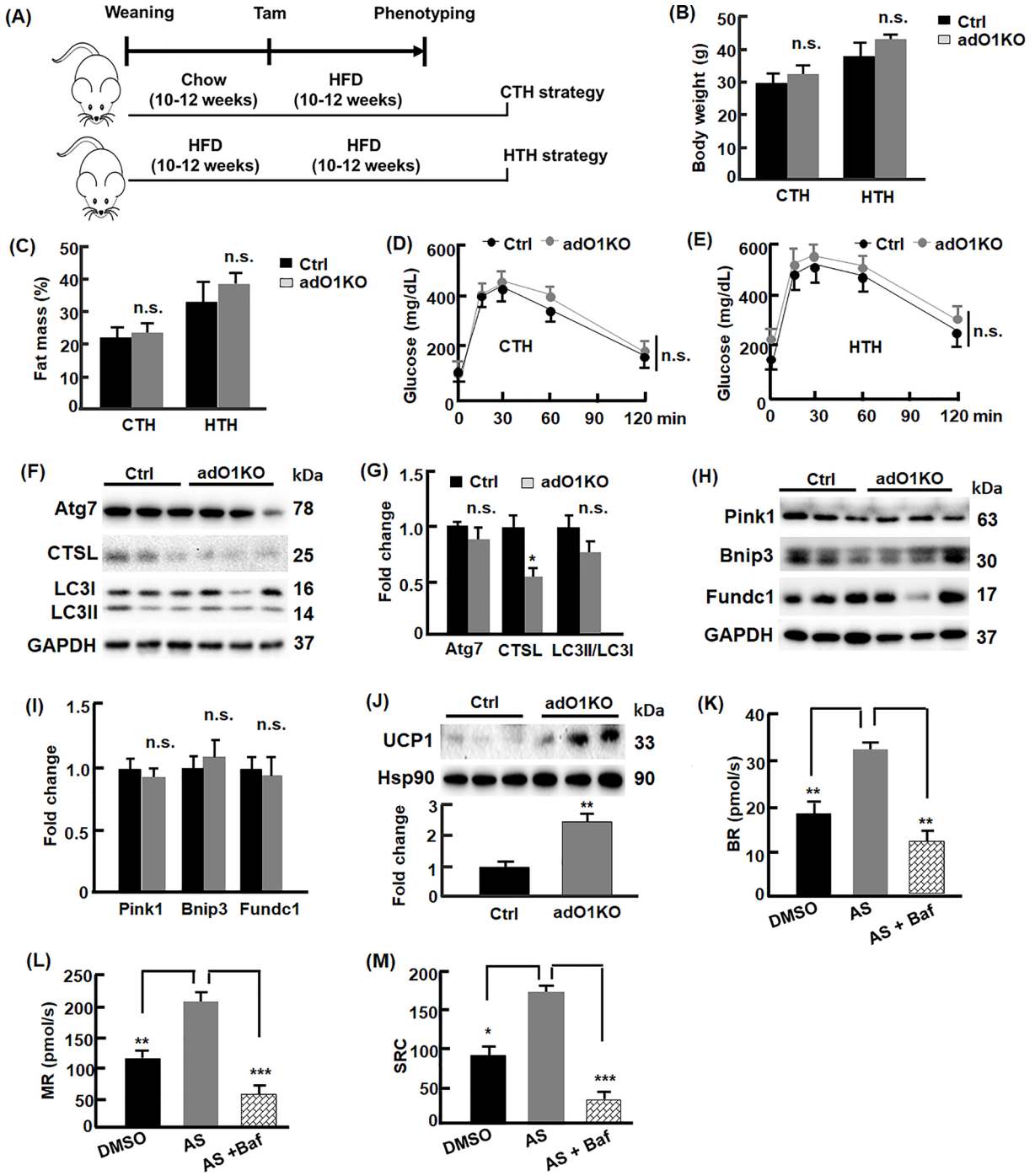

Figure 4. HFD disrupts autophagy and overrides the effects of adO1KO-induced adipose browning

(**A**) The strategies of dietary and tamoxifen treatments; CTH stands for chow→ tamoxifen→HFD, and HTH stands for HFD→ tamoxifen→HFD. (**B**) Measurements of body weight after the control and adO1KO mice were treated by CTH and HTH; n=8–12. (**C**) Measurements of fat mass after the control and adO1KO mice were treated by CTH and HTH; n=8–12. (**D,E**) Glucose tolerance test for the control and adO1KO mice treated by CTH (D) and HTH (E); n=6. (**F,G**) Western blotting (F) and densitometric (G) analyses of autophagy proteins in inguinal adipose tissues from CTH-treated mice; n=6. (**H,I**) Western blotting (H) and densitometric (I) analyses of mitophagy adaptor (Pink1) and receptors (Bnip3 and Fundc1) in inguinal adipose tissues from CTH-treated mice; n=6. (**J**) Western blotting (upper panel) and densitometric (lower panel) analyses of adipose browning maker UCP1 in inguinal adipose tissues from CTH-treated mice; n=6. (**K–M**) Measurement of basal respiration (BR, K), maximal respiration (MR, L), and spare respiration capacity (SRC, M) of 3T3L1 adipocytes treated with vehicle DMSO, FoxO1 inhibitor AS, and autophagy inhibitor Baf (i.e., bafilomycin A1); n=3–4; $^{*}P<0.05$, $^{**}P<0.01$, $^{***}P<0.001$; n.s., not significant.

Clinical Science (2024) **138** 371–385
https://doi.org/10.1042/CS20230973

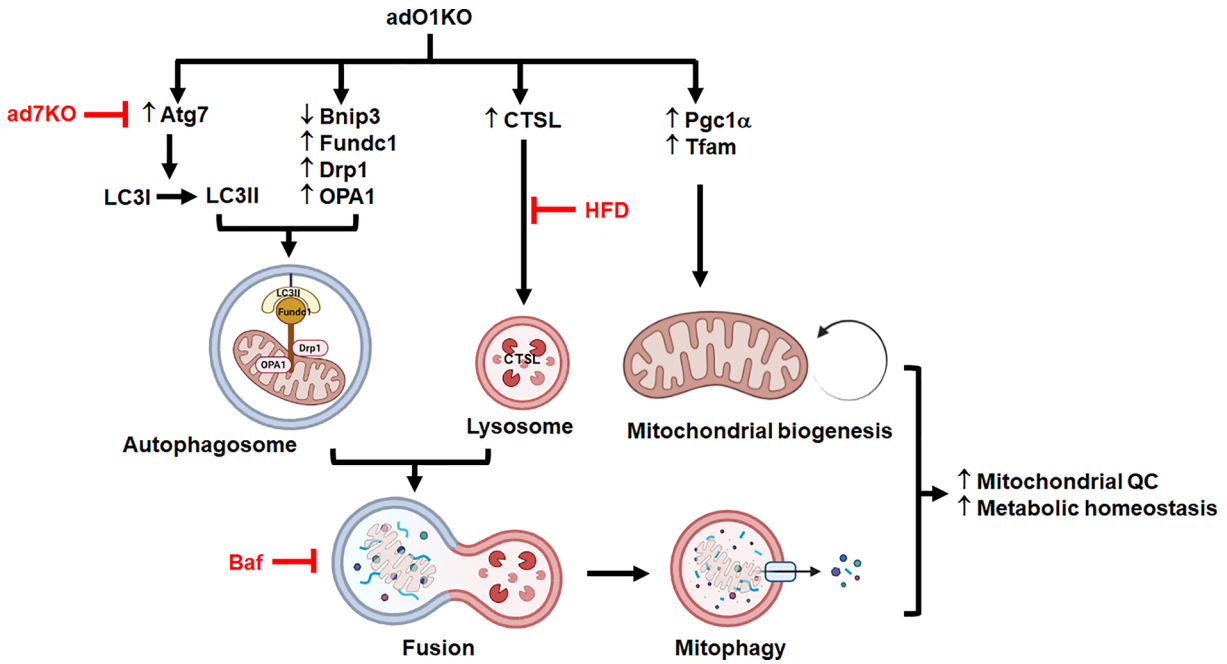

Figure 5. Proposed mechanism by which loss of FoxO1 activates alternate mechanism to maintain mitochondrial turnover and quality control

Post-developmental deletion of FoxO1 unexpectedly up-regulates Atg7 and CTSL, concurrent with elevated Fundc1 (mitophagy receptor) and Pgc1α (inducer of mitochondrial biogenesis), which sustains mitochondrial turnover and promotes mitochondrial function and metabolic health. Blockage of Atg7 (by KD or KO), CTSL (by HFD), or autophagosome–lysosome fusion (by Bafilomycin A1, shortened as Baf), compromises mitochondrial function and metabolic health.

enhancement induced by silencing FoxO1 (Figure 4K–M). Thus, autophagy-mediated mitochondrial turnover and quality control are critical for healthy browning of adipose tissue.

Discussion

The roles of FoxO transcription factors in autophagy have been observed in various tissues, such as the liver, brain, kidney, and intervertebral disk and cartilage [17]. Blockage of FoxO1 or autophagy suppresses adipogenesis [13,14]. In the present study, we discovered that silencing FoxO1 reciprocally regulated mitophagy receptors Bnip3 and Fundc1, sustaining mitophagy and mitochondrial quality control during adipose browning. In contrast with Bnip3 that was down-regulated, post-developmental ablation of FoxO1 induced Fundc1, Atg7, and CTSL (Figure 5). Mitochondrial dynamics proteins Drp1 and OPA1, which were shown to facilitate Fundc1-dependent mitophagy, were elevated significantly in adO1KO mice. In addition, adO1KO stimulated the key regulators of mitochondrial biogenesis (Pgc1α and Tfam) (Figures 1 and 2). These changes were associated with a well-sustained mitochondrial turnover and function, a healthy browning phenotype, and improved metabolic health in mice on chow diet (Figures 1 and 2 and 5). By contrast, silencing Fundc1 and Pgc1α reversed mitochondrial enhancement induced by FoxO1 inhibitor (Figure 2H,I). Blockage of autophagy by genetic (Atg7 knockout or knockdown) and pharmacological (Baf) approaches impaired mitochondrial and metabolic functions regardless of the increased mitochondrial content and browning marker (Figures 3-5). Our study suggests that healthy browning of adipose tissue requires a fine-tuned mitochondrial turnover and function.

During autophagy, lysosomes are fused with autophagosome to form autolysosomes for cargo clearance [6,52]. Lysosome dysfunction may impair autophagy machinery and activity [40,53]. In comparison to healthy lean controls, HFD-induced obese mice show a significant accumulation of phospholipids in the lysosomes, concurrent with impaired autophagic activity in the kidneys; this phenotype was recapitulated in obese human patients [53]. Dysfunctional lysosomes were also found in the adipose tissues from HFD-induced obese mice, where lysosomal enzyme CTSL was suppressed and autophagic clearance was impaired [40]. We found that adO1KO induced CTSL and autophagy in mice on chow diet (Figures 1 and 2), but HFD down-regulated CTSL and abolished adO1KO-induced

metabolic benefits (Figures 4 and 5). In addition, we observed the activation of FoxO3 via deacetylation (known as a stress indicator [48,49,54]) in adO1KO mice on HFD but not on chow diet (Supplementary Figure S4), supporting the notion that HFD and lipotoxicity constitute stress conditions [12,40,53]. The activation of FoxO3 may compensate for the loss of FoxO1, thereby abolishing the adO1KO-induced benefits (Figures 4 and 5), in that FoxO1 and FoxO3 are redundant regulators of autophagy and mitochondria [6,16,17]. Therefore, the strategies designed to rescue lysosome function (e.g., CTSL) and silencing both FoxO transcription factors may have the potential to prevent HFD-induced metabolic disorders.

The relationship of autophagy with metabolic health is complex. While ablation of autophagy in liver promotes metabolic syndrome [55], muscle specific deletion of Atg7 protected mice from obesity and insulin resistance [11]. However, systemic Atg7 or autophagy deficiency in mice compromises the adaptation to metabolic stress and promotes the progression from obesity to diabetes [56], and humans with Atg7 variants develop complex neurodevelopmental disorders with brain, muscle, and endocrine involvement [57]. In adipose tissue, aP2-Cre driven embryonic deletion of Atg7 reduces fat mass and protects mice from diet-induced obesity and insulin resistance, but the mice had a pronounced mortality rate at young age [13,14]. Recognizing the potential of off-target DNA recombination by aP2Cre, recent studies employed the adipocyte-specific adipoq-Cre to delete autophagy genes, showing that disruption of adipocyte autophagy leads to metabolic disorders [12,58–61]. Particularly, post-developmental deletion of autophagy genes *Atg3* and *Atg16L1* from adipocytes causes accumulation of dysfunctional mitochondria and systemic insulin resistance in mice fed on regular chow diet [12]. Our study reveals a novel mechanism by which adO1KO mice adopt an alternate pathway by suppressing Bnip3 but activating Fundc1 pathways along with up-regulating Atg7 and CTSL, which maintains mitochondrial turnover and metabolic health in mice on chow diet. FoxO1 may activate or repress target genes or proteins through transcriptional, post-transcriptional, and post-translational mechanisms [6,17]. Mapping of the promoter sequences revealed one or more FoxO1 binding motifs, TG(A)TTTG(T), in the related genes such as *Atg7*, *Ctsl*, *Dnm1l*, *Opa1*, *Bnip3*, and *Fundc1* (data not shown). It will be of interest for future studies to delineate how FoxO1 ablation mechanistically mediates the expression of the above-mentioned genes involved in mitophagy.

Adipose tissues acquire browning phenotype in responses to stimuli such as cold exposure and β-adrenergic stimulation [2,62]. In line with adO1KO inducing adipose browning, we found that β3-AR agonist (CL316243) and cold exposure downregulated FoxO1 (ref [2]., and data not shown). As adipose browning is hallmarked by an elevated UCP1, the protein that regulates mitochondrial proton conductance and reaction oxygen species (ROS) production in adipose tissues [63,64], researchers have been examining whether ROS plays a role in browning activity [62,65–68]. Our study suggests that adO1KO-induced browning was associate with marginal changes in ROS or oxidative stress (data not shown), consistent with the elevated UCP1 in adO1KO mice (Figure 1D,E) and the notion that UCP1 tunes down ROS to maintain redox homeostasis [62,67]. Indeed, ablation of UCP1 increases ROS and oxidative stress, abolishing the metabolic improvements induces by cold exposure [62,67]. Recently, it was shown that ROS elevation in brown adipocytes due to the lack of glucose-6-phosphate dehydrogenase impaired UCP1 expression and adaptive thermogenesis in response to cold exposure and β-adrenergic stimulation [66]. Down-regulation of ROS by overexpressing mitochondrial superoxide dismutase (SOD2) has no effect on UCP1 activity [65] although a study shows that ROS may affect UCP1 via Cys253 sulfenylation [68]. These studies support the notion that UCP1 is elevated to hold ROS in check during adipose browning in response to cold exposure and β-adrenergic stimulation, and a feedback loop for ROS to regulate UCP1 activity may exist but warrant additional investigations for validation [69].

As calorie restriction or fasting slows down aging and improves metabolic health, the potential role of fasting in adipose browning has been of interest to the research community [70–73]. Intriguingly, ROS was increased despite up-regulated UCP1 and SOD2 in adipocytes or adipose tissue in mice under starvation or nutrient restriction [70]. The elevated UCP1 and SOD2 may result from fasting-induced activation of FoxO1 [70]. However, comparative studies of human and mouse adipose tissues show that fasting suppresses FoxO1 or has marginal effects on FoxO1, respectively [72]. In addition, fasting seems to prevent adipose browning by stimulating switch from subcutaneous fat ('good' fat) to visceral fat ('bad' fat) [71]. Although fasting was proposed to mediate adipose browning by shaping gut microbiota and its metabolites [73], microbiota depletion has no effect on adaptive thermogenesis or even promotes browning of white adipose tissue during cold exposure [74,75]. The discrepancies underscore the need of further investigations to advance our understanding of adipose browning in the context of fasting and a potential role of FoxO1 in this process.

In conclusion, our data reveal a novel mechanism of reprogramed mitochondrial quality control that enhances mitochondrial function and adipose browning in adO1KO mice. Deletion of FoxO1 in adipocyte differentially regulates Bnip3 and Fundc1/Drp1/OPA1 cascade, in parallel with up-regulation of autophagy proteins Atg7 and CTSL, which sustains mitophagic activity. In addition, adO1KO stimulates mitochondrial biogenesis via the Pgc1α/Tfam

Clinical Science (2024) **138** 371–385
https://doi.org/10.1042/CS20230973

pathway. Blockage of mitophagy or mitochondrial biogenesis impairs mitochondrial function and metabolic health even in the presence of browning phenotype (e.g., elevated UCP1). Therefore, a healthy browning of white adipose tissue requires normal or robust mitochondrial quality control.

Clinical perspectives

- Browning of adipose tissue is associated with mitochondrial changes. It remains unclear how mitochondrial quality control is regulated during adipose browning.
- Post-developmental deletion of FoxO1 induces adipose browning, concurrent with sustained mitophagy (up-regulation of Fundc1 and downregulation of Bnip3) and activated mitochondrial biogenesis via Pgc1α for quality control. Blocking mitochondrial autophagy or mitochondrial biogenesis impairs mitochondrial function and metabolism, resulting in metabolic derangements regardless of a browning phenotype.
- These results reveal that a healthy browning of adipose tissue depends on fine-tuned mitochondrial quality control, shedding light on the controversial observations in the literature that target autophagy for adipose browning and obesity prevention.

Data Availability

The data will be available on reasonable request.

Competing Interests

The authors declare that there are no competing interests associated with the manuscript.

Funding

This work was supported in part by the American Heart Association [grant number 18TPA34230082 (to Z.C.)] and the USDA National Institute of Food and Agriculture [grant number 1020373 (to Z.C)].

Open Access

Open access for this article was enabled by the participation of University of Florida in an all-inclusive *Read & Publish* agreement with Portland Press and the Biochemical Society under a transformative agreement with Individual.

CRediT Author Contribution

Limin Shi: Data curation, Formal analysis, Validation, Investigation, Visualization, Writing—original draft, Project administration, Writing—review & editing. **Jinying Yang:** Data curation, Formal analysis, Validation, Investigation, Visualization, Writing—original draft, Writing—review & editing. **Zhipeng Tao:** Data curation, Formal analysis, Investigation, Visualization, Writing—original draft, Writing—review & editing. **Louise Zheng:** Data curation, Formal analysis, Investigation, Writing—original draft, Writing—review & editing. **Tyler Bui:** Investigation, Visualization. **R. Lucas Alonso:** Investigation, Visualization. **Feng Yue:** Validation, Writing—review & editing. **Zhiyong Cheng:** Conceptualization, Data curation, Formal analysis, Supervision, Funding acquisition, Validation, Investigation, Visualization, Writing—original draft, Project administration, Writing—review & editing.

Acknowledgements

Figures 2C and 5 were created with BioRender.

Abbreviations

Atg3, autophagy-related 3; Atg7, autophagy-related 7; Atg16L1, autophagy-related 16 like 1; Bnip3, Bcl-2-interacting protein 3; CTSL, Cathepsin L; Drp1, dynamin-related protein 1; FoxO1, forkhead box O1; Fundc1, FUN14 domain-containing protein 1; GAPDH, Glyceraldehyde-3-phosphate dehydrogenase; LC3, Microtubule-associated protein light chain 3; LC3I, cytosolic form of LC3; LC3II, LC3-phosphatidylethanolamine conjugate; Mfn1, mitofusin 1; Mfn2, mitofusin 2; OPA1, optic atrophy 1; Pgc1α, peroxisome proliferator-activated receptor-γ coactivator-1α; Pink1, PTEN-induced kinase 1; Tfam, mitochondrial transcription factor A.

References

1 Sakers, A., De Siqueira, M.K., Seale, P. and Villanueva, C.J. (2022) Adipose-tissue plasticity in health and disease. *Cell* **185**, 419–446, https://doi.org/10.1016/j.cell.2021.12.016
2 Shi, L., Tao, Z., Zheng, L., Yang, J., Hu, X., Scott, K. et al. (2023) FoxO1 regulates adipose transdifferentiation and iron influx by mediating Tgfbeta1 signaling pathway. *Redox Biol.* **63**, 102727, https://doi.org/10.1016/j.redox.2023.102727
3 Sidossis, L.S., Porter, C., Saraf, M.K., Borsheim, E., Radhakrishnan, R.S., Chao, T. et al. (2015) Browning of subcutaneous white adipose tissue in humans after severe adrenergic stress. *Cell Metab.* **22**, 219–227, https://doi.org/10.1016/j.cmet.2015.06.022
4 Qiu, Y., Sun, L.Z., Hu, X.L., Zhao, X., Shi, H.Y., Liu, Z. et al. (2020) Compromised browning plasticity of primary subcutaneous adipocytes derived from overweight Chinese adults. *Diabetol. Metabolic Syndrome* **12**, 91, https://doi.org/10.1186/s13098-020-00599-z
5 Carey, A.L., Formosa, M.F., Van Every, B., Bertovic, D., Eikelis, N., Lambert, G.W. et al. (2013) Ephedrine activates brown adipose tissue in lean but not obese humans. *Diabetologia* **56**, 147–155, https://doi.org/10.1007/s00125-012-2748-1
6 Cheng, Z. (2022) FoxO transcription factors in mitochondrial homeostasis. *Biochem. J.* **479**, 525–536, https://doi.org/10.1042/BCJ20210777
7 van der Bliek, A.M. (2016) Mitochondria just wanna have FUN(DC1). *EMBO J.* **35**, 1365–1367, https://doi.org/10.15252/embj.201694759
8 Chan, D.C. (2020) Mitochondrial dynamics and its involvement in disease. *Annu. Rev. Pathol.-Mech.* **15**, 235–259, https://doi.org/10.1146/annurev-pathmechdis-012419-032711
9 Heinonen, S., Buzkova, J., Muniandy, M., Kaksonen, R., Ollikainen, M., Ismail, K. et al. (2015) Impaired mitochondrial biogenesis in adipose tissue in acquired obesity. *Diabetes* **64**, 3135–3145, https://doi.org/10.2337/db14-1937
10 Sanchez, A.M., Bernardi, H., Py, G. and Candau, R.B. (2014) Autophagy is essential to support skeletal muscle plasticity in response to endurance exercise. *Am. J. Physiol. Regul. Integr. Regul. Integr. Comp. Physiol.* **307**, R956–R969, https://doi.org/10.1152/ajpregu.00187.2014
11 Kim, K.H., Jeong, Y.T., Oh, H., Kim, S.H., Cho, J.M., Kim, Y.N. et al. (2013) Autophagy deficiency leads to protection from obesity and insulin resistance by inducing Fgf21 as a mitokine. *Nat. Med.* **19**, 83–92, https://doi.org/10.1038/nm.3014
12 Cai, J., Pires, K.M., Ferhat, M., Chaurasia, B., Buffolo, M.A., Smalling, R. et al. (2018) Autophagy ablation in adipocytes induces insulin resistance and reveals roles for lipid peroxide and Nrf2 signaling in adipose-liver crosstalk. *Cell Rep.* **25**, 1708e1705–1717e1705, https://doi.org/10.1016/j.celrep.2018.10.040
13 Zhang, Y., Goldman, S., Baerga, R., Zhao, Y., Komatsu, M. and Jin, S. (2009) Adipose-specific deletion of autophagy-related gene 7 (atg7) in mice reveals a role in adipogenesis. *Proc. Natl. Acad. Sci.* **106**, 19860–19865, https://doi.org/10.1073/pnas.0906048106
14 Singh, R., Xiang, Y., Wang, Y., Baikati, K., Cuervo, A.M., Luu, Y.K. et al. (2009) Autophagy regulates adipose mass and differentiation in mice. *J. Clin. Invest.* **119**, 3329–3339, https://doi.org/10.1172/JCI39228
15 Altshuler-Keylin, S., Shinoda, K., Hasegawa, Y., Ikeda, K., Hong, H., Kang, Q. et al. (2016) Beige adipocyte maintenance is regulated by autophagy-induced mitochondrial clearance. *Cell Metab.* **24**, 402–419, https://doi.org/10.1016/j.cmet.2016.08.002
16 Tao, Z. and Cheng, Z. (2023) Hormonal regulation of metabolism-recent lessons learned from insulin and estrogen. *Clin. Sci. (Lond.)* **137**, 415–434, https://doi.org/10.1042/CS20210519
17 Cheng, Z. (2019) The FoxO-autophagy axis in health and disease. *Trends Endocrinol. Metab.* **30**, 658–671, https://doi.org/10.1016/j.tem.2019.07.009
18 Cheng, Z., Guo, S., Copps, K., Dong, X., Kollipara, R., Rodgers, J.T. et al. (2009) Foxo1 integrates insulin signaling with mitochondrial function in the liver. *Nat. Med.* **15**, 1307–1311, https://doi.org/10.1038/nm.2049
19 O-Sullivan, I., Zhang, W., Wasserman, D.H., Liew, C.W., Liu, J., Paik, J. et al. (2015) FoxO1 integrates direct and indirect effects of insulin on hepatic glucose production and glucose utilization. *Nat. Commun.* **6**, 7079, https://doi.org/10.1038/ncomms8079
20 Nakae, J., Cao, Y., Oki, M., Orba, Y., Sawa, H., Kiyonari, H. et al. (2008) Forkhead transcription factor FoxO1 in adipose tissue regulates energy storage and expenditure. *Diabetes* **57**, 563–576, https://doi.org/10.2337/db07-0698
21 Paik, J.H., Kollipara, R., Chu, G., Ji, H., Xiao, Y., Ding, Z. et al. (2007) FoxOs are lineage-restricted redundant tumor suppressors and regulate endothelial cell homeostasis. *Cell* **128**, 309–323, https://doi.org/10.1016/j.cell.2006.12.029
22 Komatsu, M., Waguri, S., Ueno, T., Iwata, J., Murata, S., Tanida, I. et al. (2005) Impairment of starvation-induced and constitutive autophagy in Atg7-deficient mice. *J. Cell Biol.* **169**, 425–434, https://doi.org/10.1083/jcb.200412022
23 Sassmann, A., Offermanns, S. and Wettschureck, N. (2010) Tamoxifen-inducible Cre-mediated recombination in adipocytes. *Genesis* **48**, 618–625, https://doi.org/10.1002/dvg.20665
24 Imai, T., Jiang, M., Chambon, P. and Metzger, D. (2001) Impaired adipogenesis and lipolysis in the mouse upon selective ablation of the retinoid X receptor alpha mediated by a tamoxifen-inducible chimeric Cre recombinase (Cre-ERT2) in adipocytes. *Proc. Ncatl. Acad. Sci.* **98**, 224–228, https://doi.org/10.1073/pnas.011528898
25 Shi, L., Tao, Z. and Cheng, Z. (2023) Assessing the activity of transcription factor FoxO1. *Methods Mol. Biol.* **2594**, 97–106, https://doi.org/10.1007/978-1-0716-2815-7˙8
26 Cero, C., Lea, H.J., Zhu, K.Y., Shamsi, F., Tseng, Y.H. and Cypess, A.M. (2021) beta3-Adrenergic receptors regulate human brown/beige adipocyte lipolysis and thermogenesis. *Jci Insight* **6**, e139160, https://doi.org/10.1172/jci.insight.139160
27 Sakamuru, S., Li, X., Attene-Ramos, M.S., Huang, R.L., Lu, J.M., Shou, L. et al. (2012) Application of a homogenous membrane potential assay to assess mitochondrial function. *Physiol. Genomics* **44**, 495–503, https://doi.org/10.1152/physiolgenomics.00161.2011
28 Schottl, T., Kappler, L., Braun, K., Fromme, T. and Klingenspor, M. (2015) Limited mitochondrial capacity of visceral versus subcutaneous white adipocytes in male C57BL/6N mice. *Endocrinology* **156**, 923–933, https://doi.org/10.1210/en.2014-1689
29 Brand, M.D. and Nicholls, D.G. (2011) Assessing mitochondrial dysfunction in cells. *Biochem. J.* **435**, 297–312, https://doi.org/10.1042/BJ20110162
30 Guo, S., Copps, K.D., Dong, X., Park, S., Cheng, Z., Pocai, A. et al. (2009) The Irs1 branch of the insulin signaling cascade plays a dominant role in hepatic nutrient homeostasis. *Mol. Cell. Biol.* **29**, 5070–5083, https://doi.org/10.1128/MCB.00138-09

Clinical Science (2024) **138** 371–385
https://doi.org/10.1042/CS20230973

31 Mather, K. (2009) Surrogate measures of insulin resistance: of rats, mice, and men. *Am. J. Physiol. Endocrinol. Metab.* **296**, E398–E399
32 Liu, X.Y., Wei, D.G. and Li, R.S. (2022) Capsaicin induces ferroptosis of NSCLC by regulating SLC7A11/GPX4 signaling in vitro. *Sci. Rep.* **12**, 11996, https://doi.org/10.1038/s41598-022-16372-3
33 Ma, S., Dubin, A.E., Zhang, Y., Mousavi, S.A.R., Wang, Y., Coombs, A.M. et al. (2021) A role of PIEZO1 in iron metabolism in mice and humans. *Cell* **184**, 969e913–982e913, https://doi.org/10.1016/j.cell.2021.01.024
34 Jeffery, E., Berry, R., Church, C.D., Yu, S., Shook, B.A., Horsley, V. et al. (2014) Characterization of Cre recombinase models for the study of adipose tissue. *Adipocyte* **3**, 206–211, https://doi.org/10.4161/adip.29674
35 Wang, Q.A., Scherer, P.E. and Gupta, R.K. (2014) Improved methodologies for the study of adipose biology: insights gained and opportunities ahead. *J. Lipid Res.* **55**, 605–624, https://doi.org/10.1194/jlr.R046441
36 Lee, K.Y., Russell, S.J., Ussar, S., Boucher, J., Vernochet, C., Mori, M.A. et al. (2013) Lessons on conditional gene targeting in mouse adipose tissue. *Diabetes* **62**, 864–874, https://doi.org/10.2337/db12-1089
37 Lynes, M.D., Schulz, T.J., Pan, A.J. and Tseng, Y.H. (2015) Disruption of insulin signaling in Myf5-expressing progenitors leads to marked paucity of brown fat, but normal muscle development. *Endocrinology* **156**, 1637–1647, https://doi.org/10.1210/en.2014-1773
38 Sanchez-Gurmaches, J. and Guertin, D.A. (2014) Adipocytes arise from multiple lineages that are heterogeneously and dynamically distributed. *Nat. Commun.* **5**, 4099, https://doi.org/10.1038/ncomms5099
39 Collier, J.J., Suomi, F., Olahova, M., McWilliams, T.G. and Taylor, R.W. (2021) Emerging roles of ATG7 in human health and disease. *EMBO Mol. Med.* **13**, e14824, https://doi.org/10.15252/emmm.202114824
40 Mizunoe, Y., Sudo, Y., Okita, N., Hiraoka, H., Mikami, K., Narahara, T. et al. (2017) Involvement of lysosomal dysfunction in autophagosome accumulation and early pathologies in adipose tissue of obese mice. *Autophagy* **13**, 642–653, https://doi.org/10.1080/15548627.2016.1274850
41 Nagakannan, P. and Eftekharpour, E. (2017) Differential redox sensitivity of cathepsin B and L holds the key to autophagy-apoptosis interplay after Thioredoxin reductase inhibition in nutritionally stressed SH-SY5Y cells. *Free Radical Biol. Med.* **108**, 819–831, https://doi.org/10.1016/j.freeradbiomed.2017.05.005
42 Palikaras, K., Lionaki, E. and Tavernarakis, N. (2018) Mechanisms of mitophagy in cellular homeostasis, physiology and pathology. *Nat. Cell Biol.* **20**, 1013–1022, https://doi.org/10.1038/s41556-018-0176-2
43 Xian, H. and Liou, Y.C. (2021) Functions of outer mitochondrial membrane proteins: mediating the crosstalk between mitochondrial dynamics and mitophagy. *Cell Death Differ.* **28**, 827–842, https://doi.org/10.1038/s41418-020-00657-z
44 Chen, M., Chen, Z.H., Wang, Y.Y., Tan, Z., Zhu, C.Z., Li, Y.J. et al. (2016) Mitophagy receptor FUNDC1 regulates mitochondrial dynamics and mitophagy. *Autophagy* **12**, 689–702, https://doi.org/10.1080/15548627.2016.1151580
45 Yang, W.B., Yan, H., Pan, Q., Shen, J.Z., Zhou, F.H., Wu, C.D. et al. (2019) Glucagon regulates hepatic mitochondrial function and biogenesis through FOXO1. *J. Endocrinol.* **241**, 265–278, https://doi.org/10.1530/JOE-19-0081
46 Yan, D., Cai, Y., Luo, J.R., Liu, J.J., Li, X., Ying, F. et al. (2020) FOXO1 contributes to diabetic cardiomyopathy via inducing imbalanced oxidative metabolism in type 1 diabetes. *J. Cell. Mol. Med.* **24**, 7850–7861, https://doi.org/10.1111/jcmm.15418
47 Mizushima, N., Yoshimori, T. and Levine, B. (2010) Methods in mammalian autophagy research. *Cell* **140**, 313–326, https://doi.org/10.1016/j.cell.2010.01.028
48 Brunet, A., Sweeney, L.B., Sturgill, J.F., Chua, K.F., Greer, P.L., Lin, Y. et al. (2004) Stress-dependent regulation of FOXO transcription factors by the SIRT1 deacetylase. *Science* **303**, 2011–2015, https://doi.org/10.1126/science.1094637
49 Wang, F., Nguyen, M., Qin, F.X. and Tong, Q. (2007) SIRT2 deacetylates FOXO3a in response to oxidative stress and caloric restriction. *Aging Cell.* **6**, 505–514, https://doi.org/10.1111/j.1474-9726.2007.00304.x
50 Klionsky, D.J., Elazar, Z., Seglen, P.O. and Rubinsztein, D.C. (2008) Does bafilomycin A1 block the fusion of autophagosomes with lysosomes? *Autophagy* **4**, 849–850, https://doi.org/10.4161/auto.6845
51 Mauvezin, C. and Neufeld, T.P. (2015) Bafilomycin A1 disrupts autophagic flux by inhibiting both V-ATPase-dependent acidification and Ca-P60A/SERCA-dependent autophagosome-lysosome fusion. *Autophagy* **11**, 1437–1438, https://doi.org/10.1080/15548627.2015.1066957
52 Tao, Z., Aslam, H., Parke, J., Sanchez, M. and Cheng, Z. (2022) Mechanisms of autophagic responses to altered nutritional status. *J. Nutr. Biochem.* **103**, 108955, https://doi.org/10.1016/j.jnutbio.2022.108955
53 Yamamoto, T., Takabatake, Y., Takahashi, A., Kimura, T., Namba, T., Matsuda, J. et al. (2017) High-fat diet-induced lysosomal dysfunction and impaired autophagic flux contribute to lipotoxicity in the kidney. *J. Am. Soc. Nephrol.* **28**, 1534–1551, https://doi.org/10.1681/ASN.2016070731
54 Ferguson, D., Shao, N., Heller, E., Feng, J., Neve, R., Kim, H.D. et al. (2015) SIRT1-FOXO3a regulate cocaine actions in the nucleus accumbens. *J. Neurosci.* **35**, 3100–3111, https://doi.org/10.1523/JNEUROSCI.4012-14.2015
55 Yang, L., Li, P., Fu, S., Calay, E.S. and Hotamisligil, G.S. (2010) Defective hepatic autophagy in obesity promotes ER stress and causes insulin resistance. *Cell Metabolism* **11**, 467–478, https://doi.org/10.1016/j.cmet.2010.04.005
56 Lim, Y.M., Lim, H., Hur, K.Y., Quan, W., Lee, H.Y., Cheon, H. et al. (2014) Systemic autophagy insufficiency compromises adaptation to metabolic stress and facilitates progression from obesity to diabetes. *Nat. Commun.* **5**, 4934, https://doi.org/10.1038/ncomms5934
57 Collier, J.J., Guissart, C., Olahova, M., Sasorith, S., Piron-Prunier, F., Suomi, F. et al. (2021) Developmental consequences of defective ATG7-mediated autophagy in humans. *New Engl. J. Med.* **384**, 2406–2417, https://doi.org/10.1056/NEJMoa1915722
58 Song, W., Postoak, J.L., Yang, G., Guo, X., Pua, H.H., Bader, J. et al. (2023) Lipid kinase PIK3C3 maintains healthy brown and white adipose tissues to prevent metabolic diseases. *Proc. Natl. Acad. Sci.* **120**, e2214874120, https://doi.org/10.1073/pnas.2214874120
59 Richter, F.C., Friedrich, M., Kampschulte, N., Piletic, K., Alsaleh, G., Zummach, R. et al. (2023) Adipocyte autophagy limits gut inflammation by controlling oxylipin and IL-10. *EMBO J.* **42**, e112202, https://doi.org/10.15252/embj.2022112202
60 Jin, Y., Ji, Y., Song, Y., Choe, S.S., Jeon, Y.G., Na, H. et al. (2021) Depletion of adipocyte Becn1 leads to lipodystrophy and metabolic dysregulation. *Diabetes* **70**, 182–195, https://doi.org/10.2337/db19-1239

61 Son, Y., Cho, Y.K., Saha, A., Kwon, H.J., Park, J.H., Kim, M. et al. (2020) Adipocyte-specific Beclin1 deletion impairs lipolysis and mitochondrial integrity in adipose tissue. *Mol. Metab.* **39**, 101005, https://doi.org/10.1016/j.molmet.2020.101005
62 Stier, A., Bize, P., Habold, C., Bouillaud, F., Massemin, S. and Criscuolo, F. (2014) Mitochondrial uncoupling prevents cold-induced oxidative stress: a case study using UCP1 knockout mice. *J. Exp. Biol.* **217**, 624–630
63 Dlaskova, A., Clarke, K.J. and Porter, R.K. (2010) The role of UCP 1 in production of reactive oxygen species by mitochondria isolated from brown adipose tissue. *Biochim. Biophys. Acta* **1797**, 1470–1476, https://doi.org/10.1016/j.bbabio.2010.04.008
64 Oelkrug, R., Kutschke, M., Meyer, C.W., Heldmaier, G. and Jastroch, M. (2010) Uncoupling protein 1 decreases superoxide production in brown adipose tissue mitochondria. *J. Biol. Chem.* **285**, 21961–21968, https://doi.org/10.1074/jbc.M110.122861
65 Silva, J.P., Shabalina, I.G., Dufour, E., Petrovic, N., Backlund, E.C., Hultenby, K. et al. (2005) SOD2 overexpression: enhanced mitochondrial tolerance but absence of effect on UCP activity. *EMBO J.* **24**, 4061–4070, https://doi.org/10.1038/sj.emboj.7600866
66 Sohn, J.H., Ji, Y., Cho, C.Y., Nahmgoong, H., Lim, S., Jeon, Y.G. et al. (2021) Spatial Regulation of Reactive Oxygen Species via G6PD in Brown Adipocytes Supports Thermogenic Function. *Diabetes* **70**, 2756–2770, https://doi.org/10.2337/db21-0272
67 Kazak, L., Chouchani, E.T., Stavrovskaya, I.G., Lu, G.Z., Jedrychowski, M.P., Egan, D.F. et al. (2017) UCP1 deficiency causes brown fat respiratory chain depletion and sensitizes mitochondria to calcium overload-induced dysfunction. *Proc. Natl. Acad. Sci.* **114**, 7981–7986, https://doi.org/10.1073/pnas.1705406114
68 Chouchani, E.T., Kazak, L., Jedrychowski, M.P., Lu, G.N.Z., Erickson, B.K., Szpyt, J. et al. (2016) Mitochondrial ROS regulate thermogenic energy expenditure and sulfenylation of UCP1. *Nature* **532**, 112–+, https://doi.org/10.1038/nature17399
69 Nicholls, D.G. and Rial, E. (2016) A novel regulatory mechanism for the brown-fat uncoupling protein? *Nat. Struct. Mol. Biol.* **23**, 364–365, https://doi.org/10.1038/nsmb.3221
70 Lettieri Barbato, D., Tatulli, G., Aquilano, K. and Ciriolo, M.R. (2015) Mitochondrial Hormesis links nutrient restriction to improved metabolism in fat cell. *Aging* **7**, 869–881, https://doi.org/10.18632/aging.100832
71 Ding, H., Zheng, S., Garcia-Ruiz, D., Hou, D., Wei, Z., Liao, Z. et al. (2016) Fasting induces a subcutaneous-to-visceral fat switch mediated by microRNA-149-3p and suppression of PRDM16. *Nat. Commun.* **7**, 11533, https://doi.org/10.1038/ncomms11533
72 Defour, M., Michielsen, C.C.J.R., O'Donovan, S.D., Afman, L.A. and Kersten, S. (2020) Transcriptomic signature of fasting in human adipose tissue. *Physiol. Genomics* **52**, 451–467, https://doi.org/10.1152/physiolgenomics.00083.2020
73 Li, G., Xie, C., Lu, S., Nichols, R.G., Tian, Y., Li, L. et al. (2017) Intermittent fasting promotes white adipose browning and decreases obesity by shaping the gut microbiota. *Cell Metab.* **26**, 672e674–685e674, https://doi.org/10.1016/j.cmet.2017.08.019
74 Suarez-Zamorano, N., Fabbiano, S., Chevalier, C., Stojanovic, O., Colin, D.J., Stevanovic, A. et al. (2015) Microbiota depletion promotes browning of white adipose tissue and reduces obesity. *Nat. Med.* **21**, 1497–1501, https://doi.org/10.1038/nm.3994
75 Krisko, T.I., Nicholls, H.T., Bare, C.J., Holman, C.D., Putzel, G.G., Jansen, R.S. et al. (2020) Dissociation of adaptive thermogenesis from glucose homeostasis in microbiome-deficient mice. *Cell Metab.* **31**, 592e599–604e599, https://doi.org/10.1016/j.cmet.2020.01.012